

Nucleon electric dipole form factor in QCD vacuum

Wei-Yang Liu^{*} and Ismail Zahed[†]

*Center for Nuclear Theory, Department of Physics and Astronomy,
Stony Brook University, Stony Brook, New York 11794-3800, USA*

(Dated: January 24, 2025)

In the QCD instanton vacuum, the C-even and C-odd nucleon Pauli form factors receive a large contribution from the underlying ensemble of pseudoparticles, that is sensitive to a finite QCD vacuum angle θ . This observation is used to derive explicitly the electric dipole form factor for light quark flavors, and estimate the proton and neutron electric dipole moment induced by a small CP violating θ . The results are in the range of some recently reported lattice simulations.

I. INTRODUCTION

The resolution of the CP problem in baryogenesis is central to our understanding of baryon asymmetry in the universe [1]. CP violation in the weak sector of the standard model, proves to be orders of magnitude away from its resolution, while CP violation in the strong sector, puts its resolution within range [2].

The QCD vacuum is rich with topologically active pseudoparticles which are CP conjugated pairs (instantons and anti-instantons). They are natural sources of local CP violation effects. CP is strongly violated in QCD at finite theta angle. A reliable description of ensembles of these pseudoparticles in the semi-classical approximation, is provided by the instanton liquid model (ILM) [3–6] (and references therein). The model has proven to be very useful in capturing many aspects of most hadronic correlations both in vacuum, in hadronic states and in matter. Here, we will focus on understanding the role of these pseudoparticles in the composition of the hadronic electric dipole moment.

For many decades, the nucleon electric dipole moment has been used as a measure of the strong CP violation caused by a finite theta angle in QCD. The current empirical estimate puts its upper bound at about 10^{-26} e-cm [7]. This is an ideal task for ab-initio lattice simulations, yet the smallness of the observable makes

the task daunting in light of the signal-to-noise ratio [8, 9]. Notwithstanding this, the latest lattice estimate puts it at about $10^{-16} \theta$ e-cm for a finite theta angle [10], which would limit θ to about 10^{-10} by the empirical bound.

The QCD vacuum breaks conformal symmetry, a mechanism at the origin of most hadronic masses. Detailed gradient flow (cooling) techniques have revealed a striking semi-classical landscape made of instantons and anti-instantons, the vacuum tunneling pseudoparticles with unit topological charges [11–16]. These pseudoparticles break chiral symmetry through fermionic zero modes with fixed chirality (left or right). The key features of this landscape are [17]

$$n_{I+A} \equiv \frac{1}{R^4} \approx \frac{1}{\text{fm}^4} \quad \frac{\rho}{R} \approx \frac{1}{3} \quad (1)$$

for the instanton plus anti-instanton density and size, respectively. The hadronic scale $R = 1$ fm emerges as the mean quantum tunneling rate of the pseudoparticles. Deep in the cooling time the tunnelings are sparse, well described by the instanton liquid model (ILM) with a packing fraction

$$\kappa \equiv \pi^2 \rho^4 n_{I+A} \approx 0.1 \quad (2)$$

The main purpose of this work is to evaluate the C-odd nucleon electric dipole form factor, and provide an estimate of the proton and neutron electric dipole moments in the ILM. In section II we briefly review the salient features of the pseudoparticle fluctuations in the ILM, with a comparison to some lattice simulations.

^{*} wei-yang.liu@stonybrook.edu

[†] ismail.zahed@stonybrook.edu

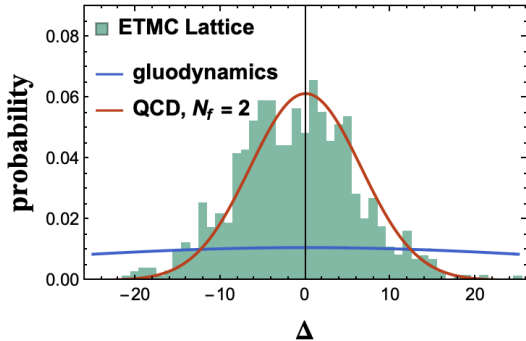


FIG. 1. The ILM results unquenched (red-solid) and quenched (blue-solid), compared to the lattice results from the ETMC collaboration [9].

In section III we define the four C-even or odd form factors associated to the electric current in the nucleon. The C-odd electric dipole form factor for each flavor contribution is evaluated in the ILM. This form factor is found to be related to the Pauli form factor. In particular, the finite proton and neutron electric dipole moments in the ILM are shown to be comparable to some recent lattice simulations. Our conclusions are in section IV. Further details can be found in the appendices.

II. QCD INSTANTON VACUUM

The size distribution of the instantons and anti-instantons density (their tunneling rate) in the vacuum is well captured semi-empirically by

$$n(\rho) \sim \frac{1}{\rho^5} (\rho \Lambda_{QCD})^b e^{-C\rho^2/R^2} \quad (3)$$

with the mean value (1). Here $b = 11N_c/3 - 2N_f/3$ (one loop), and C is a number of order 1 fixed by the binary gauge interactions among pseudoparticles in the vacuum [18, 19].

To capture the fluctuations of the number of pseudoparticles N_{\pm} , we identify them with the scalar and pseudoscalar gluonic densities in the

vacuum

$$\begin{aligned} \frac{1}{32\pi^2} \int d^4x F^2(x) &= (N_+ + N_-) = N \\ \frac{1}{32\pi^2} \int d^4x F\tilde{F}(x) &= (N_+ - N_-) = \Delta \end{aligned} \quad (4)$$

with $gF \rightarrow F$ assumed. For a random quenched vacuum with Poissonian N_{\pm} at finite angle θ ,

$$\begin{aligned} \frac{\langle F^2 \rangle_{\theta}}{32\pi^2} &\approx n_{I+A} \cos \theta \\ \frac{\langle F\tilde{F} \rangle_{\theta}}{32\pi^2} &\approx i n_{I+A} \sin \theta \end{aligned} \quad (5)$$

with the breaking of scale or conformal symmetry manifested for vanishing theta. However, in the ILM the distributions of N_{\pm} are not Poissonian. The fluctuations in the sum N follow from low-energy theorems [20]

$$\mathbb{P}(N) = e^{-\frac{b\bar{N}}{4}} \left(\frac{\bar{N}}{N} \right)^{\frac{bN}{4}} \quad (6)$$

with the vacuum topological compressibility

$$\frac{\sigma_T}{V_4} = \frac{\langle (N - \bar{N})^2 \rangle}{V_4} = \frac{4}{b} n_{I+A} \quad (7)$$

and the volume extensive mean $\bar{N} = n_{I+A} V_4$. The fluctuations in the difference Δ are fixed by the topological susceptibility [3]. At $\theta = 0$, the distribution reads

$$\mathbb{Q}(\Delta) = \frac{1}{\sqrt{2\pi\chi_t}} \exp\left(-\frac{\Delta^2}{2\chi_t}\right) \quad (8)$$

The topological susceptibility χ_t in gluodynamics is

$$\frac{\chi_t}{V_4} = \frac{\langle \Delta^2 \rangle}{V_4} \approx n_{I+A} \quad (9)$$

which is large. However, in QCD it is substantially screened by the light quarks, as illustrated in Fig. 1 with current quark mass $m = 10$ MeV. The width of the distribution reads

$$\frac{\langle \Delta^2 \rangle}{\bar{N}} \sim \left(1 + N_f \frac{m^*}{m}\right)^{-1} \quad (10)$$

Note that the topological susceptibility is sensitive to the determinantal mass m^* . The details

about how to fix the determinantal mass are given in Appendix C and in [21, 22] (and references therein).

In Fig. 1 we show the unquenched ILM results (10) (red-solid) and quenched ILM (9) (blue-solid), compared to the lattice results from the ETMC collaboration [9]. The latters used twisted mass clover-improved fermions $N_f = 2 + 1 + 1$, in a 4-volume $64^3 \times 128 a^4$ with lattice spacing $a = 0.0801(4)$ fm, and physical pion mass $m_\pi = 139$ MeV. For the ILM parameters see below.

III. NUCLEON EM FORM FACTORS

At finite vacuum angle θ , the QCD action in Euclidean signature is supplemented by the

topological term

$$\frac{\theta}{32\pi^2} \int d^4x F \tilde{F} \rightarrow \theta \Delta$$

which is at the origin of strong CP violation. In the ILM, this contribution acts as a topological chemical potential for Δ , by enhancing instantons and depleting anti-instantons. This affects most observables, and in particular the electromagnetic (EM) form factors of hadrons, as we will detail in this section.

The coupling to photon can be described by Dirac F_1 , Pauli F_2 , electric dipole moment form factor F_3 , and axial tensor form factor F_A .

$$\begin{aligned} \langle N' | J_{\text{EM}}^\mu = \sum_f Q_f \bar{\psi}_f \gamma^\mu \psi_f | N \rangle \\ = \bar{u}_{s'}(P') \left[\gamma^\mu F_1(Q^2) + \frac{i\sigma^{\mu\nu} q_\nu}{2M_N} (F_2(Q^2) - i\gamma^5 F_3(Q^2)) + \frac{1}{M_N^2} (\not{q} q^\mu - q^2 \gamma^\mu) \gamma^5 F_A(Q^2) \right] u_s(P) \end{aligned} \quad (11)$$

with the Sachs FFs $G_{C,M}$

$$\begin{aligned} G_C(Q^2) &= F_1(Q^2) + \frac{Q^2}{4M_N^2} F_2(Q^2) \\ G_M(Q^2) &= F_1(Q^2) + F_2(Q^2) \end{aligned} \quad (12)$$

and the electric dipole and axial-tensor FFs $G_{D,A}$

$$\begin{aligned} G_D(Q^2) &= F_3(Q^2) \\ G_A(Q^2) &= F_A(Q^2) \end{aligned} \quad (13)$$

with the two latters vanishing for $\theta = 0$. The magnetic and electric dipole moment are defined respectively,

$$\mu_N = G_M(0)e/2M_N \quad d_N = F_3(0)e/2M_N \quad (14)$$

For finite theta, (11) will be organized through

$$J_\mu^{\text{Dirac}}(q, \theta) + J_\mu^{\text{Pauli}}(q, \theta) + J_\mu^A(q, \theta) \quad (15)$$

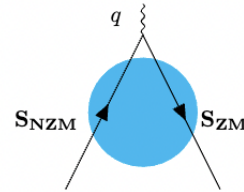


FIG. 2. Leading pseudoparticle (single instanton) contribution to the quark EM current in the ILM.

A. Emergent EM vertex

To see how the pseudoparticles contribute to the EM FF of hadrons, consider the instanton (antiinstanton) insertion to the charge current on a quark line illustrated in Fig. 2. In an instanton (antiinstanton) the incoming left-handed (right-handed) quark flips to a right-handed (left-handed) through a zero mode,

then scatters off a virtual photon before exiting through a non-zero mode, with the result for a single quark [23]. The effective interaction amplitude is defined as

$$\int d^4 z e^{-iq \cdot z} \left[S_{\text{NZM}}(x, z) \gamma^\mu S_{\text{ZM}}(z, y) + S_{\text{ZM}}(x, z) \gamma^\mu S_{\text{NZM}}(z, y) \right] \quad (16)$$

For a single instanton, the zero mode propagator is

$$S_{\text{ZM}}(x, x') = \frac{\phi_I(x) \phi_I^\dagger(x')}{im} \rightarrow \frac{\phi_I(x) \phi_I^\dagger(x')}{im^*} \quad (17)$$

with the zero modes defined in (A5). The singular $1/m$ in the single instanton approximation is shifted to finite $1/m^*$ by disordering in the ILM [4, 6, 24] (and references therein). The determinantal mass m^* is seen to follow from

the constituent mass through a similar disordering [22]

$$M_q(0) = \frac{n_{I+A}}{2N_c} \frac{4\pi^2 \rho^2}{m} \rightarrow \frac{n_{I+A}}{2N_c} \frac{4\pi^2 \rho^2}{m^*} \quad (18)$$

with the identification

$$m^* = \sqrt{\frac{n_{I+A}}{2N_c}} \left(\sqrt{2} \|q\varphi'^2\| \right) \quad (19)$$

The norm uses the zero mode profile $\varphi'(q)$ defined as

$$\varphi'(q) = \pi \rho^2 \left(I_0 K_0(z) - I_1 K_1(z) \right)'_{z=\rho q/2} \quad (20)$$

The typical value of the constituent mass is about $M_q(0) \approx 380 - 395$ MeV [6, 21, 25].

Inserting (17) into (16) yield the instanton induced effective EM vertex

$$V_+^\mu(x, y) = \int d^4 z_I dU_I \int d^4 z e^{-iq \cdot z} \left[\bar{S}_{nz}^{(I)}(x - z_I, z - z_I) \gamma^\mu \frac{\phi_I(z - z_I) \phi_I^\dagger(y - z_I)}{im^*} + \frac{\phi_I(x - z_I) \phi_I^\dagger(z - z_I)}{im^*} \gamma^\mu S_{nz}^{(I)}(z - z_I, y - z_I) \right] \frac{1 + \gamma^5}{2} \quad (21)$$

The effective vertex for the anti-instanton $V_-^\mu(x, y)$ follows by interchanging $\tau_\mu^- \leftrightarrow \tau_\mu^+$,

$\sigma_\mu \leftrightarrow \bar{\sigma}_\mu$, and $\gamma^5 \leftrightarrow -\gamma^5$. Now the effective quark operator can be written as

$$\int \frac{d^4 k}{(2\pi)^4} \frac{d^4 k'}{(2\pi)^4} \bar{\psi}(k') \left[\frac{N_+}{V} V_+(k', k) + \frac{N_-}{V} V_-(k', k) \right] \psi(k) \quad (22)$$

The on-shell reduction of the in-out quark lines can be obtained by using the large time asymptotics as detailed in appendix B2. More specifically, the on-shell reduction of the emergent vertex is ($q^2 = -Q^2 < 0$)

$$V_+(k', k) = \lim_{\substack{x_4 \rightarrow +\infty \\ y_4 \rightarrow -\infty}} \left[\int d^3 \vec{x} d^3 \vec{y} e^{ik' \cdot x} i\gamma_4 V_+^\mu(x, y) i\gamma_4 e^{-ik \cdot y} \right]_{\substack{ik_4 = |\vec{k}| \\ ik'_4 = |\vec{k}'|}} \quad (23)$$

with the result for the Pauli contribution

$$V_\pm(k', k) \simeq i(2\pi)^4 \delta(k - k' + q) \frac{8\pi^2 \rho^4}{N_c} \frac{1 \mp \gamma^5}{2} \frac{i\sigma^{\mu\nu} q_\nu}{2m^*} \times \int_0^1 dt \left[tK_0(u\sqrt{1-t}) - \frac{1}{8} \frac{\sqrt{1-t}}{u} \frac{\partial}{\partial u} (uK_1(u\sqrt{1-t})) \right] \Big|_{u=\rho Q} \quad (24)$$

where $K_n(x)$ is the modified Bessel function of the second kind.

B. f -quark EDM

At zero vacuum angle, the Pauli contribution to the charge form factor in (15), receives a large contribution from pseudoparticles in the QCD instanton vacuum [23]. We now show that this observation carries to the CP-odd contributions at finite vacuum angle. The Pauli part of the form factor of a quark of flavor f is then

$$J_{\mu,f}^{\text{Pauli}}(q, \theta) = Q_f e F_I(\rho Q) \bar{u}_s(k') \left(\frac{N_+}{\bar{N}} \frac{1 - \gamma^5}{2} \frac{i\sigma_{\mu\nu} q_\nu}{2m^*} + \frac{N_-}{\bar{N}} \frac{1 + \gamma^5}{2} \frac{i\sigma_{\mu\nu} q_\nu}{2m^*} \right) u_s(k) \quad (25)$$

with the pseudoparticle induced form factor

$$F_I(q) = \frac{8\pi^2 \rho^4 n_{I+A}}{N_c} \frac{1}{q^2} \left[\left(2 - 2qK_1(q) \right) - \left(\frac{7}{q^2} - \frac{7}{4}qK_1(q) - \frac{7}{2}K_2(q) \right) \right] \quad (26)$$

The first parenthesis is identical to the Kochelev's computation using an on-shell limit [23]. The additional contribution in our case stems from use of the large Euclidean time approximation in the on-shell reduction scheme discussed in Appendix B. The latter is more appropriate for Euclidean formulations [26].

The averaging of (25) over N_\pm is carried using the grand-canonical ensemble detailed in appendix D, with the result

$$\langle J_{\mu,f}^{\text{Pauli}}(q, \theta) \rangle = Q_f e F_I(\rho Q) \bar{u}_s(k') \left(1 - \frac{\langle \Delta^2 \rangle_c}{\bar{N}} \theta i\gamma^5 \right) \frac{i\sigma_{\mu\nu} q_\nu}{2m^*} u_s(k) \quad (27)$$

where we have used $\langle N_\pm \rangle = \bar{N} \pm i\langle \Delta^2 \rangle_c \theta$

It approaches to the asymptotic form in the large momentum transfer limit $q \rightarrow \infty$. Here $\langle \Delta^2 \rangle_c = \chi_t$ is the vacuum connected topological susceptibility (10). A comparison of (26) to (11) yields the pseudoparticle contribution to the $F_{2,3}$ f -quark form factors

$$\begin{aligned} F_2^f(Q^2) &\rightarrow Q_f e F_I(\rho Q) \\ F_3^f(Q^2) &\rightarrow Q_f e F_I(\rho Q) \frac{\langle \Delta^2 \rangle_c}{\bar{N}} \theta \end{aligned} \quad (28)$$

in leading order in the density. Note that our result for the CP even F_2^f form factor is different from the one in [23] which is IR singular. The reason is that our use of the large time asymptotic method presented in appendix B 2 is more appropriate for the on-shell reduction in Euclidean space as emphasized in [26]. The logarithmic sensitivity of the CP even F_2^f form

factor, will be fixed by the magnetic moment (see below).

Inserting (26) in (13) yields the f -quark electric dipole moment

$$\frac{F_3^f(Q^2)}{\theta} = \left(1 + N_f \frac{m^*}{m} \right)^{-1} F_2^f(Q^2) \quad (29)$$

for small vacuum angle. The numerical result is sensitive to the value of the emergent determinantal mass m^* given in (19).

C. Proton and neutron EDM

In the ILM, the proton and neutron are strongly correlated quark-diquark states, with a tight scalar-iso-scalar diquark $[ud]_S$ and weaker axial-vector flavor-triplet diquark $[ud]_A$ [4]. This strong correlation in the scalar channel follows from the particle-anti-particle symmetry

TABLE I. proton and neutron EDM.

| | Neutron ($10^{-3} e\theta\cdot\text{fm}$) | Proton ($10^{-3} e\theta\cdot\text{fm}$) | Ratio $ d_n/d_p $ |
|-------------------------|---|--|------------------------|
| ILM | $d_n = -4.73$ | $d_p = 4.44$ | 1.067 |
| Faccioli et al. [27] | $ d_n = 6 \sim 14$ | – | – |
| ChPT [28] | $ d_n = 2.10$ | $ d_p = 2.38$ | 0.882 |
| χQCD [10] | $d_n = -1.48^{+0.14}_{-0.31}$ | $d_p = 3.8^{+1.1}_{-0.8}$ | $0.39^{+0.12}_{-0.12}$ |
| Bhattacharya et al.[29] | $d_n = -3^{+7}_{-20}$ | $d_p = 24^{+10}_{-30}$ | $0.13^{+0.80}_{-0.30}$ |
| Dragos et al. [30] | $d_n = -1.52 \pm 0.71$ | $d_p = 1.1 \pm 1.0$ | 1.4 ± 1.4 |
| ETMC[9] | $ d_n = 0.9 \pm 2.4$ | – | – |

between the spin-0 pion and the spin-0 diquark. To take advantage of this observation, the pro-

ton and neutron SU(6) wavefunctions can be repacked in quark-diquark contributions [31] (and references therein)

$$\begin{aligned}
p \uparrow &= \frac{1}{\sqrt{18}} \left(3[ud]_S u \uparrow + 2[uu]_A^+ d \downarrow - \sqrt{2}[uu]_A^0 d \uparrow - \sqrt{2}[ud]_A^+ u \downarrow + [ud]_A^0 u \uparrow \right) \\
n \uparrow &= \frac{1}{\sqrt{18}} \left(3[ud]_S d \uparrow + 2[dd]_A^+ u \downarrow - \sqrt{2}[dd]_A^0 u \uparrow - \sqrt{2}[ud]_A^+ d \downarrow + [ud]_A^0 d \uparrow \right)
\end{aligned} \tag{30}$$

with the upper labels $0, \pm$ referring to the vector helicities. We can use (30) to evaluate the individual flavor contributions to the CP-odd contribution to the Pauli form factor. For that we note in the ILM the non-zero mode insertion

can only happen on the unpaired quark, as the paired quarks in a diquark are locked by zero modes only.

Alternatively, we may use (29) to derive the CP-odd contribution in a proton and neutron through the Pauli form factor, hence

$$\begin{aligned}
\frac{d_p(0)}{\theta} &= \left(1 + N_f \frac{m^*}{m} \right)^{-1} \times \left(\mu_p - Q_p \frac{e}{2M_N} \right) \\
\frac{d_n(0)}{\theta} &= \left(1 + N_f \frac{m^*}{m} \right)^{-1} \times \left(\mu_n - Q_n \frac{e}{2M_N} \right)
\end{aligned} \tag{31}$$

(27), (29) and (31) are the main results of this work.

Using the empirical values $\mu_p = 2.793 e/2M_N \simeq 0.2937 e\cdot\text{fm}$ and $\mu_n = -1.913 e/2M_N \simeq -0.2012 e\cdot\text{fm}$ [32], the

electric dipole moments read

$$\begin{aligned}
\frac{d_p(0)}{e\theta} &= +0.004436 \text{ fm} \\
\frac{d_n(0)}{e\theta} &= -0.004732 \text{ fm}
\end{aligned} \tag{32}$$

with a fixed ratio $d_p(0)/d_n(0) = -0.9373$. The comparison to the recently reported lattice results and chiral perturbation calculation

(ChPT) for the nucleon EDM are given in Table I, with $N_f = 2$, $m = 8.0$ MeV and $m^* = 110.7$ MeV. Overall, our results appear to be in the range of some of the proton and neutron EDM reported by some lattice collaborations. For completeness, we note an earlier estimate of the neutron dipole moment $|d_n(0)| = (6-14) \times 10^{-3}$ ($e\theta \cdot \text{fm}$) using a numerical ensemble of pseudo-particles to describe the ILM, with a moment approximation to extract the EDM [27].

In Fig. 3 we show our result for the C-odd neutron electric dipole form factor (solid-red band) at low Q^2 . The logarithmic infrared sensitivity of the induced pseudo-particle form factor in (26), is cutoff around $1 \text{ fm}^{-1} \simeq 0.1973$ GeV (constant red dashed line) as we start to probe multi-pseudoparticle correlations, well beyond our current single instanton approach in the dilute ILM description. The momentum dependence is compared to the reported lattice C-odd electric dipole form factor (blue data) from the χ QCD lattice collaboration [10]. The green band is their estimated extrapolation using linear fits, and the yellow band is their estimated extrapolation using a square fit with additional Q^4 term. The lattice simulations are carried out using overlap fermions, in a 4-volume 64×24^3 ensemble with a lattice spacing $a = 0.1105$ fm.

IV. CONCLUSIONS

In QCD, the breaking of conformal symmetry puts stringent constraints on the bulk hadronic correlations in the form of low energy theorems [20]. These constraints are enforced in the QCD instanton vacuum in the form of stronger than Poisson fluctuations in the number of pseudoparticles, with a vacuum compressibility indicative of a quantum liquid. The fluctuations in the difference of the pseudoparticles are peaked around neutral topological charge with the variance, which is fixed by the topological susceptibility which is large in gluodynamics, but substantially screened in

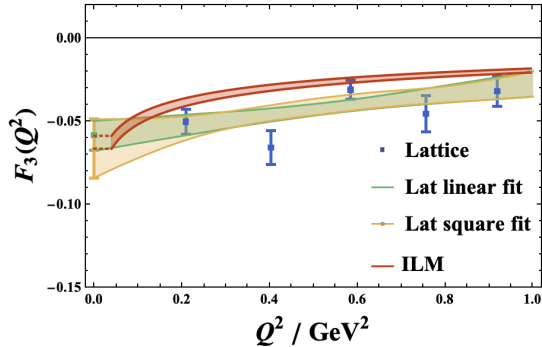


FIG. 3. The C-odd electric dipole form factor from the ILM (solid-red) with $F_3(0)$ value normalized to the lattice linear and square fit. The Q^2 dependence is compared to the lattice results (blue data) from the χ QCD collaboration [10] with $m_\pi = 339$ MeV. The green band is a lattice linear fit and the yellow band is a lattice square fit with additional Q^4 term

QCD. These are essential features of the ILM.

In the ILM, the Pauli form factor of constituent quarks receive a large contribution in the ILM, correcting an early observation in [23]. In the presence of a CP violation by a small vacuum angle θ , we have shown that an axial contribution develops in the Pauli form factor, driven mostly by the vacuum topological susceptibility. We have used this result to estimate the induced the electric dipole moment in both the proton and neutron, as well as the semi-hard momentum dependence of the Pauli form factors F_2 , F_3 induced by the pseudoparticles. Our results are in the range of recently reported lattice results extrapolated at the physical pion mass [10].

Acknowledgements

We thank Fangcheng He for some discussions. This work is supported by the Office of Science, U.S. Department of Energy under Contract No. DE-FG-88ER40388. This research is also supported in part within the framework of the Quark-Gluon Tomography (QGT) Topical Collaboration, under contract no. DE-SC0023646.

Appendix A: Quark propagator in the single instanton background

In singular gauge, the instanton gauge field is given by

$$A_\mu^a(x; \Omega_I) = -\frac{1}{g} R^{ab}(U_I) \bar{\eta}_{\mu\nu}^b \partial_\nu \ln \Pi(x - z_I) \quad (\text{A1})$$

Here the instanton moduli is captured by $\Omega_I = (z_I, \rho, U_I)$ the rigid color rotation U_I , instanton location z_I and size ρ , with the singular gauge potential

$$\Pi(x) = 1 + \frac{\rho^2}{x^2} \quad (\text{A2})$$

The rigid color rotation

$$R^{ab}(U_I) = \frac{1}{2} \text{Tr}(\tau^a U_I \tau^b U_I^\dagger)$$

is defined with τ^a as an $N_c \times N_c$ matrix with 2×2 Pauli matrices embedded in the upper left corner. For the anti-instanton field, we substitute $\bar{\eta}_{\mu\nu}^a$ by $\eta_{\mu\nu}^a$ and flip the sign in front of Levi-Cevita tensor, $\epsilon_{\mu\nu\rho\lambda} \rightarrow -\epsilon_{\mu\nu\rho\lambda}$.

The effects of the quark masses on the quark propagator in the instanton or antiinstanton fields, are not known in closed form [26]. However, for small masses, the propagator can be

$$\Delta_I(x, y) = \frac{1}{4\pi^2(x-y)^2} \left(1 + \rho^2 \frac{x_\mu y_\nu}{x^2 y^2} U_I \tau_\mu^- \tau_\nu^+ U_I^\dagger \right) \frac{1}{\Pi(x)^{1/2} \Pi(y)^{1/2}} \quad (\text{A7})$$

The location of the instanton z_I is set to be zero for simplicity and can be recovered by transla-

expanded around the chiral limit

$$\begin{aligned} S_I(x, y) &= \langle x | \frac{1}{i\not{\partial} + \not{A}_I + im} | y \rangle \\ &= S_{\text{ZM}}^{(I)}(x, y) + S_{\text{NZM}}^{(I)}(x, y) + \mathcal{O}(m) \end{aligned} \quad (\text{A3})$$

The zero mode propagator reads

$$S_{\text{ZM}}^{(I)}(x, y) = \frac{\phi_I(x) \phi_I^\dagger(y)}{im} \quad (\text{A4})$$

where the left-handed zero mode in singular gauge is

$$\phi_I(x) = \left(\frac{\rho}{\pi|x|(x^2 + \rho^2)^{3/2}} \right) \not{x} \frac{1 - \gamma^5}{2} U_I \chi \quad (\text{A5})$$

with χ , a color-spin locked 4-spinor.

The non-zero mode propagator in the chiral-split form reads [33]

$$\begin{aligned} S_{\text{NZM}}^{(I)}(x, y) &= i \overrightarrow{\not{D}}_x \Delta_I(x, y) \frac{1 + \gamma^5}{2} + \Delta_I(x, y) i \overleftarrow{\not{D}}_y \frac{1 - \gamma^5}{2} \\ &= S_{nz}^{(I)}(x, y) \frac{1 + \gamma^5}{2} + \bar{S}_{nz}^{(I)}(x, y) \frac{1 - \gamma^5}{2} \end{aligned} \quad (\text{A6})$$

where $\psi(x) \overleftarrow{\not{D}}_\mu = (-\partial_\mu - iA_\mu) \psi(x)$. The massless scalar propagator in the single instanton background field is defined as [33]

tional symmetry $x \rightarrow x - z_I$ and $y \rightarrow y - z_I$. After a few steps of algebraic calculation, $S_{nz}^{(I)}$ and $\bar{S}_{nz}^{(I)}$ can be recast in the form [4, 26, 34]

$$\begin{aligned} S_{nz}^{(I)}(x, y) &= \left[\frac{-i(\not{x} - \not{y})}{2\pi^2(x-y)^4} \left(1 + \rho^2 \frac{x_\mu y_\nu}{x^2 y^2} U_I \tau_\mu^- \tau_\nu^+ U_I^\dagger \right) - \frac{\rho^2 \gamma_\mu}{4\pi^2} \frac{x_\rho(x-y)_\nu y_\lambda}{(x^2 + \rho^2)x^2(x-y)^2 y^2} U_I \tau_\rho^- \tau_\mu^+ \tau_\nu^- \tau_\lambda^+ U_I^\dagger \right] \\ &\quad \times \frac{1}{\Pi(x)^{1/2} \Pi(y)^{1/2}} \end{aligned} \quad (\text{A8})$$

and

$$\begin{aligned} \bar{S}_{nz}^{(I)}(x, y) &= \left[\frac{-i(\not{x} - \not{y})}{2\pi^2(x-y)^4} \left(1 + \rho^2 \frac{x_\mu y_\nu}{x^2 y^2} U_I \tau_\mu^- \tau_\nu^+ U_I^\dagger \right) - \frac{\rho^2 \gamma_\mu}{4\pi^2} \frac{x_\rho(x-y)_\nu y_\lambda}{(y^2 + \rho^2)x^2(x-y)^2 y^2} U_I \tau_\rho^- \tau_\nu^+ \tau_\mu^- \tau_\lambda^+ U_I^\dagger \right] \\ &\times \frac{1}{\Pi(x)^{1/2} \Pi(y)^{1/2}} \end{aligned} \quad (\text{A9})$$

Note that the propagator $S_{\text{NZM}}^{(A)}$ for the anti-instanton can be obtained via the substitutions $\tau_\mu^- \leftrightarrow \tau_\mu^+$, and $\gamma^5 \leftrightarrow -\gamma^5$.

Appendix B: Reduction scheme

The on-shell reduction of the Euclidean and massless quark propagator in the instanton background is subtle. In principle, it can be achieved in two ways: 1/ through LSZ reduc-

tion in the zero momentum limit; 2/ through the long term "time" asymptotic. Here we will quote both procedures, although the long time asymptotics is the one that turns out to be IR free in most cases [26].

1. Zero Euclidean momentum

For massless quarks, the LSZ reduction in the zero momentum ($k^2 \ll Q^2$) limit reads

$$\int d^4 y e^{-ik \cdot y} S_{nz}(x, y) \not{k} \psi_L(k) \simeq \frac{e^{-ik \cdot x}}{(1 + \rho^2/x^2)^{1/2}} \left[1 + (1 - e^{ik \cdot x}) \frac{\rho^2}{2x^2} \frac{x_\mu k_\nu}{k \cdot x} U \tau_\mu^- \tau_\nu^+ U^\dagger \right] \psi_L(k) \quad (\text{B1})$$

$$\int d^4 y e^{ik \cdot y} \bar{\psi}_R(k) \not{k} \bar{S}_{nz}(y, x) \simeq \frac{e^{ik \cdot x}}{(1 + \rho^2/x^2)^{1/2}} \left[1 + (1 - e^{-ik \cdot x}) \frac{\rho^2}{2x^2} \frac{k_\mu x_\nu}{k \cdot x} U \tau_\mu^- \tau_\nu^+ U^\dagger \right] \bar{\psi}_R(k) \quad (\text{B2})$$

In the asymptotic limit $x^2 \gg \rho^2$, the reduction yields an on-shell free quark.

the large Euclidean "time" asymptotics, to put the quark on mass shell, a common procedure on the lattice. More specifically, we have

2. Large Euclidean time

The alternative reduction scheme that proves to be IR safe in most cases, consists in taking

$$\begin{aligned} &\lim_{\tau \rightarrow -\infty} i \int d^3 \vec{y} S_{nz}(x, y) e^{i\vec{k} \cdot \vec{y}} \left[\gamma_4 \psi_L(k) e^{-|\vec{k}| \tau} \right] \\ &= \frac{e^{-ik \cdot x}}{(1 + \rho^2/x^2)^{1/2}} \left[1 - i \frac{\rho^2}{2x^2} x_\mu k_\nu U \tau_\mu^- \tau_\nu^+ U^\dagger \int_0^1 dt e^{i(1-t)k \cdot x} \right. \\ &\quad \left. + i \frac{\rho^2}{4x^2(x^2 + \rho^2)} \frac{x_\mu \gamma_\nu \gamma_4}{|\vec{k}|} x_\rho k_\lambda U \tau_\mu^- \tau_\nu^+ \tau_\rho^- \tau_\lambda^+ U^\dagger \int_0^1 dt e^{i(1-t)k \cdot x} + \frac{\rho^2}{2x^2(x^2 + \rho^2)} \frac{x_\mu \gamma_\nu \gamma_4}{|\vec{k}|} U \tau_\mu^- \tau_\nu^+ U^\dagger \right] \psi_L(k) \end{aligned} \quad (\text{B3})$$

$$\begin{aligned}
& \lim_{\tau \rightarrow \infty} i \int d^3 \vec{y} \left[\bar{\psi}_R(k) \gamma_4 e^{|\vec{k}| \tau} \right] \bar{S}_{nz}(y, x) e^{-i \vec{k} \cdot \vec{y}} \\
&= \frac{e^{i \vec{k} \cdot x}}{(1 + \rho^2/x^2)^{1/2}} \bar{\psi}_R(k) \left[1 + i \frac{\rho^2}{2x^2} k_\mu x_\nu U \tau_\mu^- \tau_\nu^+ U^\dagger \int_0^1 dt t e^{-i(1-t)k \cdot x} \right. \\
&\quad \left. - i \frac{\rho^2}{4x^2(x^2 + \rho^2)} \frac{\gamma_4 \gamma_\nu}{|\vec{k}|} k_\lambda x_\rho x_\mu U \tau_\lambda^- \tau_\rho^+ \tau_\nu^- \tau_\mu^+ U^\dagger \int_0^1 dt e^{-i(1-t)k \cdot x} + \frac{\rho^2}{2x^2(x^2 + \rho^2)} \frac{\gamma_4 \gamma_\mu x_\nu}{|\vec{k}|} U \tau_\mu^- \tau_\nu^+ U^\dagger \right] \quad (\text{B4})
\end{aligned}$$

where we have used the fact that

$$\frac{1}{2} \left(1 - \frac{\vec{\sigma} \cdot \vec{k}}{|\vec{k}|} \right) \psi_L(k) = \psi_L(k)$$

and

$$\frac{1}{2} \left(1 + \frac{\vec{\sigma} \cdot \vec{k}}{|\vec{k}|} \right) \psi_R(k) = \psi_R(k)$$

Combined with the reduction scheme in large Euclidean time, (23) reads

$$\begin{aligned}
V_+(k', k) &= - \frac{2\rho^2}{N_c m^*} \int d^4 x e^{-iq \cdot x} \left\{ \frac{e^{i \vec{k}' \cdot x}}{(x^2 + \rho^2)^2} \frac{1}{8} \text{Tr}_c \left[\left(1 + i \frac{\rho^2}{2x^2} k'_\sigma x_\nu \tau_\sigma^- \tau_\nu^+ \int_0^1 dt t e^{-i(1-t)k' \cdot x} \right. \right. \right. \\
&\quad \left. \left. - i \frac{\rho^2}{4x^2(x^2 + \rho^2)} \frac{\gamma_4 \gamma_\sigma}{|\vec{k}|} k'_\nu x_\rho x_\lambda \tau_\nu^- \tau_\rho^+ \tau_\sigma^- \tau_\lambda^+ \int_0^1 dt e^{-i(1-t)k' \cdot x} \right. \right. \\
&\quad \left. \left. + \frac{\rho^2}{2x^2(x^2 + \rho^2)} \frac{\gamma_4 \gamma_\sigma x_\nu}{|\vec{k}|} \tau_\sigma^- \tau_\nu^+ \right) \gamma^\mu \not{x} \gamma_\alpha \gamma_\beta \tau_\alpha^- \tau_\beta^+ \right] - \left. \begin{array}{l} h.c. \\ (k' \rightarrow k) \end{array} \right\} \quad (\text{B5})
\end{aligned}$$

Appendix C: Determinantal mass m^* in the instanton liquid

In the instanton liquid model, the concept of a determinantal mass m^* characterises the width of the zero-mode zone, a key characteristic of the spontaneous breaking of chiral symmetry. It is sampled by the ensemble average of the fermionic determinant

$$\left\langle \rho^{N N_f} \prod_f \text{Det}(\not{D})_{\text{ZM}} \right\rangle = (\rho m^*)^{N N_f} \quad (\text{C1})$$

a measure of the unquenching of the gauge configurations. In particular, a reduction in the density of pseudoparticles at low resolution

$$\frac{n_{I+A}}{2} = \int d\rho n(\rho) (m^* \rho)^{N_f} \quad (\text{C2})$$

where $n(\rho)$ denotes the quenched instanton size distribution in (3), and m^* is the determinantal mass. Numerical simulations of ensembles of interacting pseudoparticles give $m^* \sim 103 \text{ MeV}$ [35]

In the thermodynamic limit ($N, V \rightarrow \infty$ with n_{I+A} fixed) alongside the large N_c limit, the emergent instantonic vertices exponentiate, giving

$$Z_{N_\pm} \propto \int \mathcal{D}\psi \mathcal{D}\psi^\dagger \exp \left(- \int d^4 x \mathcal{L}_{\text{eff}} \right) \quad (\text{C3})$$

where the effective Lagrangian in Euclidean space reads [22]

$$\mathcal{L}_{\text{eff}} = -\psi^\dagger i \not{\partial} \psi - G_I (1 + \delta) \theta_+ - G_I (1 - \delta) \theta_- \quad (\text{C4})$$

where the vertices are defined as

$$\theta_{\pm}(x) = \int dU_I \prod_f \left[\frac{m_f}{4\pi^2 \rho^2} + i\psi_f^\dagger(x) U_I \frac{1}{8} \tau_\mu^\mp \tau_\nu^\pm \gamma_\mu \gamma_\nu U_I^\dagger \frac{1 \mp \gamma^5}{2} \psi_f(x) \right] \quad (\text{C5})$$

The emergent parameters G_I and δ are fixed by the saddle point approximation. The effective coupling G_I

$$G_I = \frac{N}{2V} \left(\frac{4\pi^2 \rho^2}{m^*} \right)^{N_f} \quad (\text{C6})$$

is tied to the mean instanton size ρ , density N/V , and determinantal mass m^* [22, 35–37]. The screened topological charge δ is

$$\delta = N_f \frac{m^* \Delta}{m N} \quad (\text{C7})$$

In the saddle point approximation, the momentum dependent constituent mass is

$$M(k) = \frac{N}{2V} \frac{k^2 \varphi'(k)^2}{m^*} \quad (\text{C8})$$

along with the gap equation which naturally determines the determinantal mass [22]

$$m^* = m + 8\pi^2 \rho^2 \int \frac{d^4 k}{(2\pi)^4} \frac{M(k) \mathcal{F}(k)}{k^2 + M^2(k)} \quad (\text{C9})$$

where the instanton-quark form factor is defined as

$$\sqrt{\mathcal{F}(k)} = z \frac{d}{dz} [I_0(z) K_0(z) - I_1(z) K_1(z)] \Big|_{z=\frac{k}{2}} \quad (\text{C10})$$

Using the instanton parameters $n_{I+A} = 1 \text{ fm}^{-4}$, $\rho = 0.313 \text{ fm}$ and the current mass $m = 8 \text{ MeV}$, the determinantal mass is

$$m^* = 102.1 \text{ MeV} \quad (\text{C11})$$

with the constituent mass of 395 MeV [6, 21, 25], and a quark condensate $-(275 \text{ MeV})^3$. The estimated determinantal mass is much closer to the numerical value of $m^* \simeq 103 \text{ MeV}$ [35].

Appendix D: Averaging in grand canonical instanton liquid ensemble

Here we briefly outline the averaging over the fluctuations in the number of pseudoparticles

in the ILM. In a grand canonical description where N_{\pm} are allowed to fluctuate, the partition function of the QCD vacuum with finite vacuum angle is written as

$$\begin{aligned} \mathcal{Z}(\mu, \theta) &= \sum_{N_+, N_-} Z_{N_{\pm}} e^{(\mu+i\theta)N_+ + (\mu-i\theta)N_-} \\ &= \exp \left(\frac{b}{4} \langle N \rangle_{\theta} e^{\frac{4\mu}{b}} \right) \end{aligned} \quad (\text{D1})$$

This partition function yield the distribution with the measures (6) and (8) at $\mu = 0$ and $\theta = 0$ or equivalently written as [3, 4, 38]

$$\mathcal{P}(N_+, N_-) = \mathbb{P}(N) \mathbb{Q}(\Delta) \quad (\text{D2})$$

with mean $\bar{N} = \langle N \rangle$ and $Q_t = \langle \Delta \rangle$. As a result, vacuum expectation values of most quarks and gluon operators are averaged through

$$\langle \mathcal{O} \rangle = \sum_{N_+, N_-} \mathcal{P}(N_+, N_-) \langle \mathcal{O} \rangle_{N_{\pm}} \equiv \overline{\langle \mathcal{O} \rangle}_{N_{\pm}} \quad (\text{D3})$$

The averaging is carried out over the configurations with fixed N_{\pm} (canonical ensemble average), followed by an ensemble averaging over the distribution (8).

Similarly, the evaluation of the hadronic matrix elements can be formulated as a large- T reduction of a 3-point function

$$\frac{\langle h | \mathcal{O} | h \rangle}{\langle h | h \rangle} = \lim_{T \rightarrow \infty} \frac{\langle J_h^\dagger(T/2) \mathcal{O} J_h(-T/2) \rangle_{\text{con}}}{\langle J_h^\dagger(T/2) J_h(-T/2) \rangle} \quad (\text{D4})$$

where $J_h(t)$ is a pertinent source for the hadronic state h .

Now with this grand canonical framework, the insertion of the gluonic scalar operator and topological charge operator in the the connected correlation function can be carried out by

$$\frac{1}{32\pi^2} \left\langle \mathcal{O} \int d^4x F_{\mu\nu} F_{\mu\nu} \right\rangle_{\text{con}} = (\langle N^2 \rangle - \langle N \rangle^2) \frac{\partial}{\partial N} \langle \mathcal{O} \rangle_{N\pm} \Big|_{\substack{N=\bar{N} \\ \Delta=0}} \quad (\text{D5})$$

$$\frac{1}{32\pi^2} \left\langle \mathcal{O} \int d^4x F_{\mu\nu} \tilde{F}_{\mu\nu} \right\rangle_{\text{con}} = \langle \Delta^2 \rangle \frac{\partial}{\partial \Delta} \langle \mathcal{O} \rangle \Big|_{\substack{N=\bar{N} \\ \Delta=0}} \quad (\text{D6})$$

The quark contribution are usually penalized by $1/N_c$ -counting, as they are rooted in the quark-instanton interaction. Therefore, in this

case, the leading contribution will come from the fluctuations.

This approach can used to calculate the neutron EDM.

$$\begin{aligned} \vec{d}_N &= \langle N(\theta) | \int d^3\vec{x} \vec{x} J_0(\vec{x}) | N(\theta) \rangle \\ &\simeq -i\theta \langle N(0) | \int d^3\vec{x} \vec{x} J_0(\vec{x}) \left(\frac{1}{32\pi^2} \int d^4z F_{\mu\nu} \tilde{F}_{\mu\nu} \right) | N(0) \rangle \end{aligned} \quad (\text{D7})$$

In the $1/N_c$ book-keeping, the dominant contributions to neutron EDM are given by

$$\vec{d}_N = -i\theta \langle \Delta^2 \rangle \frac{\partial}{\partial \Delta} \langle N | \int d^3\vec{x} \vec{x} J_0(\vec{x}) | N \rangle \Big|_{\substack{N=\bar{N} \\ \Delta=0}} \quad (\text{D8})$$

-
- [1] A. D. Sakharov, *Pisma Zh. Eksp. Teor. Fiz.* **5**, 32 (1967).
- [2] D. Kharzeev, E. Shuryak, and I. Zahed, *Phys. Rev. D* **102**, 073003 (2020), arXiv:1906.04080 [hep-ph].
- [3] D. Diakonov, M. V. Polyakov, and C. Weiss, *Nucl. Phys. B* **461**, 539 (1996), arXiv:hep-ph/9510232.
- [4] T. Schäfer and E. V. Shuryak, *Rev. Mod. Phys.* **70**, 323 (1998), arXiv:hep-ph/9610451.
- [5] M. A. Nowak, M. Rho, and I. Zahed, *Chiral nuclear dynamics* (1996).
- [6] W.-Y. Liu, (2025), arXiv:2501.07776 [hep-ph].
- [7] C. Abel *et al.*, *Phys. Rev. Lett.* **124**, 081803 (2020), arXiv:2001.11966 [hep-ex].
- [8] S. Syritsyn, T. Izubuchi, and H. Ohki, *PoS Confinement2018*, 194 (2019), arXiv:1901.05455 [hep-lat].
- [9] C. Alexandrou, A. Athenodorou, K. Hadjiyiannakou, and A. Todaro, *Phys. Rev. D* **103**, 054501 (2021), arXiv:2011.01084 [hep-lat].
- [10] J. Liang, A. Alexandru, T. Draper, K.-F. Liu, B. Wang, G. Wang, and Y.-B. Yang (χ QCD), *Phys. Rev. D* **108**, 094512 (2023), arXiv:2301.04331 [hep-lat].
- [11] D. B. Leinweber, in *Workshop on Light-Cone QCD and Nonperturbative Hadron Physics* (1999) pp. 138–143, arXiv:hep-lat/0004025.

- [12] C. Michael and P. S. Spencer, *Nucl. Phys. B Proc. Suppl.* **42**, 261 (1995), [arXiv:hep-lat/9411015](#).
- [13] C. Michael and P. S. Spencer, *Phys. Rev. D* **52**, 4691 (1995), [arXiv:hep-lat/9503018](#).
- [14] J. C. Biddle, W. Kamleh, and D. B. Leinweber, *PoS LATTICE2018*, 256 (2018), [arXiv:1903.07767 \[hep-lat\]](#).
- [15] A. Athenodorou, P. Boucaud, F. De Soto, J. Rodríguez-Quintero, and S. Zafeiropoulos, *JHEP* **02**, 140 (2018), [arXiv:1801.10155 \[hep-lat\]](#).
- [16] A. Ringwald and F. Schrempp, *Phys. Lett. B* **459**, 249 (1999), [arXiv:hep-lat/9903039](#).
- [17] E. V. Shuryak, *Nucl. Phys. B* **203**, 93 (1982).
- [18] D. Diakonov, *Proc. Int. Sch. Phys. Fermi* **130**, 397 (1996), [arXiv:hep-ph/9602375](#).
- [19] E. V. Shuryak, (1999), [arXiv:hep-ph/9909458](#).
- [20] V. A. Novikov, M. A. Shifman, A. I. Vainshtein, and V. I. Zakharov, *Nucl. Phys. B* **191**, 301 (1981).
- [21] W.-Y. Liu, E. Shuryak, and I. Zahed, (2023), [arXiv:2307.16302 \[hep-ph\]](#).
- [22] W.-Y. Liu, E. Shuryak, and I. Zahed, (2024), [arXiv:2404.03047 \[hep-ph\]](#).
- [23] N. I. Kochelev, *Phys. Lett. B* **565**, 131 (2003), [arXiv:hep-ph/0304171](#).
- [24] P. V. Pobylitsa, *Physics Letters B* **226**, 387 (1989).
- [25] W.-Y. Liu, E. Shuryak, and I. Zahed, *Phys. Rev. D* **107**, 094024 (2023), [arXiv:2302.03759 \[hep-ph\]](#).
- [26] Y. Liu and I. Zahed, (2021), [arXiv:2102.07248 \[hep-ph\]](#).
- [27] P. Faccioli, D. Guadagnoli, and S. Simula, *Phys. Rev. D* **70**, 074017 (2004), [arXiv:hep-ph/0406336](#).
- [28] E. Mereghetti, J. de Vries, W. H. Hockings, C. M. Maekawa, and U. van Kolck, *Phys. Lett. B* **696**, 97 (2011), [arXiv:1010.4078 \[hep-ph\]](#).
- [29] T. Bhattacharya, V. Cirigliano, R. Gupta, E. Mereghetti, and B. Yoon, *Phys. Rev. D* **103**, 114507 (2021), [arXiv:2101.07230 \[hep-lat\]](#).
- [30] J. Dragos, T. Luu, A. Shindler, J. de Vries, and A. Yousif, *Phys. Rev. C* **103**, 015202 (2021), [arXiv:1902.03254 \[hep-lat\]](#).
- [31] M. Anselmino, E. Predazzi, S. Ekelin, S. Fredriksson, and D. B. Lichtenberg, *Rev. Mod. Phys.* **65**, 1199 (1993).
- [32] C. Patrignani *et al.* (Particle Data Group), *Chin. Phys. C* **40**, 100001 (2016).
- [33] L. S. Brown, R. D. Carlitz, D. B. Creamer, and C. Lee, *Phys. Rev. D* **17**, 1583 (1978).
- [34] A. G. Zubkov, O. V. Dubasov, and B. O. Kerbikov, *Int. J. Mod. Phys. A* **14**, 241 (1999), [arXiv:hep-ph/9712549](#).
- [35] P. Faccioli and E. V. Shuryak, *Phys. Rev. D* **64**, 114020 (2001), [arXiv:hep-ph/0106019](#).
- [36] T. Schäfer and E. V. Shuryak, *Phys. Rev. D* **53**, 6522 (1996), [arXiv:hep-ph/9509337](#).
- [37] E. Shuryak and I. Zahed, *Phys. Rev. D* **107**, 034023 (2023), [arXiv:2110.15927 \[hep-ph\]](#).
- [38] I. Zahed, *Phys. Rev. D* **104**, 054031 (2021), [arXiv:2102.08191 \[hep-ph\]](#).